

# Knock-on Tail Observation Scenario Using VUV and VIS Spectra from Energetic Ions Produced by ${}^6\text{Li}+d$ Reaction<sup>\*)</sup>

Kento KIMURA and Hideaki MATSUURA

*Department of Applied Quantum Physics and Nuclear Engineering, Kyushu University,  
744 Motoooka, Fukuoka 819-0395, Japan*

(Received 10 January 2019 / Accepted 17 July 2019)

In the scattering process of energetic ions, the contribution of the nuclear elastic scattering (NES) appears in addition to Coulomb scattering. The NES forms a knock-on tail (non-Maxwellian tail) in ion velocity distribution functions. When the knock-on tail is formed, energy spectra of particles produced by a nuclear reaction are distorted from Gaussian distribution. The vacuum ultra violet (VUV) and visible light (VIS) emission spectra of  ${}^7\text{Li}$  produced by the  ${}^6\text{Li}+d$  reaction are broadened by the Doppler effect. Characteristics of these broadened spectra depend on the shape of ion distribution functions. Therefore, the knock-on tails on the deuteron velocity distribution function could be observed by using the Doppler effect for the VUV and VIS spectra. Because high wavelength resolution instruments ( $\sim 10$  pm in VUV,  $\sim 4$  pm in VIS) are available, detailed measurements of the size and shape of the knock-on tail by VUV and VIS spectroscopy might be possible. We evaluated the VUV and VIS spectra for the cases when a knock-on tail is formed and not formed assuming the hydrogen beam injected deuterium plasma. Clear difference of the Doppler broadening between the cases was seen. It is shown that the VUV and VIS emission spectra can be a useful tool for the knock-on tail observation.

© 2019 The Japan Society of Plasma Science and Nuclear Fusion Research

Keywords: nuclear elastic scattering, knock-on tail, deuterium plasma, VUV, VIS, Doppler broadening, atomic process

DOI: 10.1585/pfr.14.3403147

## 1. Introduction

The scattering process of energetic ions in high temperature plasmas differs from Coulomb scattering. The differential scattering cross-section of nuclear elastic scattering (NES) [1, 2] is defined by subtracting the Rutherford cross-section from the measured differential elastic scattering cross-section. Because the NES is a large angle scattering, the energetic ions transport a large amount of energy to bulk ions in a single scattering event. Consequently, knock-on tails (non-Maxwellian components) are formed in the ion velocity distribution functions [3,4]. The knock-on tail formation modifies the fusion reaction rate coefficient [5] and the neutron energy spectrum [3]. The NES always occurs and influences nuclear burning characteristics and slowing-down of energetic ions in high temperature plasmas. In  $\text{D}^3\text{He}$  plasmas, the ignition property is improved by the NES, because the slowing-down of energetic protons is underestimated when the NES is neglected [6]. In DT plasmas, an application to plasma diagnostics utilizing the neutron energy spectrum modified by the NES has been studied [3,4].

The NES effects in high temperature plasmas have been investigated numerically, and their experimental ver-

ifications are few. Thus, it is important to experimentally ascertain the knock-on tail formation to construct the database for NES effects in high temperature plasmas. The knock-on tail observation experiment using  $\gamma$ -ray generating  ${}^6\text{Li}(d,p\gamma){}^7\text{Li}^{3+}$  reaction has been proposed [7], and planned on the Large Helical Device. In the above observation experiment method, the enhancement of  $\gamma$ -ray generation rate due to the knock-on tail formation is focused. Because the  $\gamma$ -ray generation rate is evaluated as an integral quantity of the product of the velocity distribution function and the  ${}^6\text{Li}+d$  reaction cross-section, only the size of the knock-on tail can be obtained by this method. For the quantitative evaluation of NES effects, it is desirable to measure the shape and size of the fuel ion velocity distribution function. An observation method that measures the shape and size of the fuel ion velocity distribution function from the modified neutron energy spectrum and Doppler broadening of  $\gamma$ -rays has been proposed [8–10]. The energy resolution (full width at half maximum) of the neutron spectrometer used by Källne for measurement was  $\Delta E/E = 4\%$  [4]. In order to measure the fuel ion velocity distribution function with high accuracy, it is desirable to use an instrument with higher energy resolution.

Here, we focus on the vacuum ultra violet (VUV) and visible light (VIS) emission spectra of  ${}^7\text{Li}^{2+}$  produced by the  ${}^6\text{Li}+d$  reaction. The advantage of this scenario is the higher energy (wavelength) resolution of the spec-

author's e-mail: k\_kimura@nucl.kyushu-u.ac.jp

\*) This article is based on the presentation at the 27th International Toki Conference (ITC27) & the 13th Asia Pacific Plasma Theory Conference (APPTC2018).

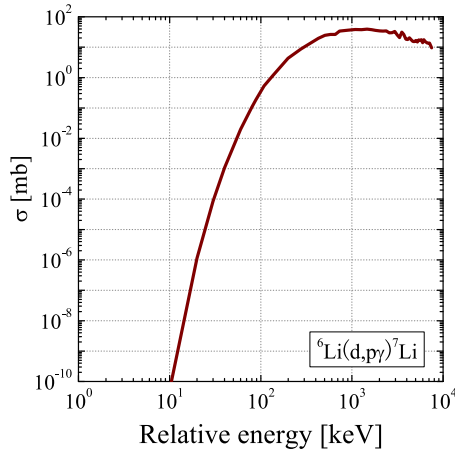


Fig. 1 Cross-section of  ${}^6\text{Li}(d,p\gamma){}^7\text{Li}$  versus relative energy of the reactants.

trometer than that of instruments measuring neutrons and  $\gamma$ -rays. Furthermore, VIS, VUV and soft X-ray spectroscopies have obtained abundant measurement results. Figure 1 plots the cross-section of the  ${}^6\text{Li}+d$  reaction as a function of relative energy of the reactants. Because the cross-section of the  ${}^6\text{Li}+d$  reaction rapidly increases with increasing the relative energy ( $< \sim 100$  keV), the reaction rate increases as a result of the existence of a small fraction of energetic component in deuteron velocity distribution function. Therefore, the  ${}^7\text{Li}^{3+}$  energy spectrum well reflects the shape and size of the knock-on tail on the deuteron velocity distribution function. The  ${}^7\text{Li}^{3+}$  energy spectrum when the knock-on tail is formed is largely different from that without the knock-on tail [8].  ${}^7\text{Li}^{3+}$  is fully ionized in the high temperature plasma and does not spontaneously emit photons. Hence, the  ${}^7\text{Li}^{3+}$  ion must be recombined in some way to observe line emission spectra. A well-known diagnostic method is charge-exchange spectroscopy [11], which supplies electrons to the target ions by a charge-exchange reaction with an injected neutral particle beam. When a fast neutral hydrogen beam is injected,  ${}^7\text{Li}^{3+}$  becomes an H-like ion by the charge-exchange reaction, and emits a line spectrum. When the knock-on tail produces a large number of energetic  ${}^7\text{Li}^{3+}$  ions, the Doppler broadening of the line spectrum of  ${}^7\text{Li}^{2+}$  increases. From the emission spectrum of  ${}^7\text{Li}^{2+}$  (measured by a spectrometer), we can infer the shape and size of the knock-on tail.

The purpose of this study is to show a possibility of Doppler broadenings of VUV and VIS emission spectra of  ${}^7\text{Li}^{2+}$  to observe the knock-on tail in the hydrogen beam injected deuterium plasma. We estimated the VUV and VIS spectra for the cases when a knock-on tail is formed and not formed. We compare the Doppler broadenings and resolutions of the current spectrometer in the VUV and VIS spectra. We focus on the VUV and VIS of the  $n = 1-2$  transition ( $\lambda = 13.50$  nm) and the  $n = 4-5$  transition ( $\lambda = 449.9$  nm), respectively. The shape and size of the

knock-on tail is expected to depend on the plasma conditions [7]. Therefore, we clarify the dependence of the Doppler broadenings on the plasma temperature and the beam energy, and investigate fundamental properties.

## 2. Analysis Model

We assumed a spatially uniform deuterium plasma. It was assumed that reactions (i.e. DD reaction,  ${}^6\text{Li}+d$  reaction, NES, charge-exchange reaction), and photon emission occur isotropically. The expected emission spectrum is expressed by the quantity per unit solid angle. The steady-state deuteron velocity distribution function  $f_d$  was evaluated by solving the Fokker-Planck equation as follows:

$$\left(\frac{\partial f_d(v_d)}{\partial t}\right)^{\text{Coulomb}} + S(v_d) - \frac{f_d(v_d)}{\tau_p} = 0, \quad (1)$$

where  $\tau_p$  is the particle confinement time. The first term on the left-hand-side of Eq. (1) is the Coulomb collision term. The second term is the source term given by [12, 13].

$$S(v_d) = 8\pi\gamma^2 n_d / v_d \int_{\gamma v_d}^{\infty} \sigma_{\text{NES}} f_p(v_p) v_p dv_p. \quad (2)$$

Here,  $\gamma = (m_p + m_d)/2m_p$ , and the subscripts p and d denote proton and deuteron, respectively.  $n_d$  represents the deuteron density.  $\gamma v_d$  is the lowest proton velocity that can change the deuteron velocity to the velocity  $v_d$  through elastic scattering. The NES cross-section  $\sigma_{\text{NES}}$  was taken from Perkins and Cullen [2]. The proton velocity distribution function  $f_p$  was assumed to be the slowing-down distribution [14]. The  ${}^7\text{Li}^{3+}$  energy spectrum was evaluated by the following formula:

$$\frac{dN_{7\text{Li}^{3+}}}{dE} = \iint f_{6\text{Li}}(v_{6\text{Li}}) f_d(v_d) \sigma_{6\text{Li}+d} \times \delta(E - E_{7\text{Li}^{3+}}) v_r dv_{6\text{Li}} dv_d, \quad (3)$$

where

$$E_{7\text{Li}^{3+}} = \frac{1}{2} m_{7\text{Li}^{3+}} |\mathbf{V}_c|^2 + \frac{m_p}{m_p + m_{7\text{Li}^{3+}}} (Q + E_r) + |\mathbf{V}_c| \cos\theta_c \sqrt{\frac{2m_p m_{7\text{Li}^{3+}}}{m_p + m_{7\text{Li}^{3+}}} (Q + E_r)}, \quad (4)$$

with,  $v_r = |\mathbf{v}_{6\text{Li}} - \mathbf{v}_d|$ .  $\mathbf{V}_c$  is the center-of-mass velocity between  ${}^6\text{Li}$  and deuteron.  $\theta_c$  is the angle between the  ${}^7\text{Li}^{3+}$  velocity in the center-of-mass frame and the center-of-mass velocity.  $Q$  is the  $Q$  value of the  ${}^6\text{Li}+d$  reaction, and  $E_r$  represents the relative energy. The cross-section of the  ${}^6\text{Li}+d$  reaction  $\sigma_{6\text{Li}+d}$  was taken from Voronchev and Kukulin [15]. We assumed a Maxwellian distribution whose temperature is equal to that of the bulk deuteron for the  ${}^6\text{Li}$  velocity distribution function. The energy spectrum of the  ${}^7\text{Li}^{2+}$  recombined by the charge-exchange reaction was calculated as

$$\frac{dN_{7\text{Li}^{2+}}}{dE_{7\text{Li}^{2+}}} = \iint f_{7\text{Li}^{3+}}(v_{7\text{Li}^{3+}}) f_{\text{H}0}(v_{\text{H}0}) \sigma_{\text{CX}} \times \delta(E_{7\text{Li}^{2+}} - E_{7\text{Li}^{3+}}) v_r dv_{7\text{Li}^{3+}} dv_{\text{H}0}, \quad (5)$$

where H0 denotes neutral hydrogen, and  $\sigma_{CX}$  is the charge-exchange reaction cross-section of H0 and  ${}^7\text{Li}^{3+}$ . The  ${}^7\text{Li}^{3+}$  velocity distribution function  $f_{7\text{Li}^{3+}}$  was evaluated giving the source term in Eq. (5). It was assumed that the neutral hydrogen density is 10% of the hydrogen beam density injected [16], and the neutral hydrogen distribution  $f_{\text{H0}}$  is monoenergy distribution. We assumed that the  ${}^7\text{Li}$  velocity vector does not change before and after charge-exchange reaction. The charge-exchange reaction cross-section was taken from the National Institute for Fusion Science database [17]. The expected photon emission spectrum of  ${}^7\text{Li}^{2+}$  was evaluated as

$$\frac{dN_{\text{photon}}}{d\lambda} = \int \frac{dN_{7\text{Li}^{2+}}}{dE_{7\text{Li}^{2+}}} \delta(E - E_{\text{photon}}) \frac{dE}{d\lambda} dE_{7\text{Li}^{2+}}, \quad (6)$$

where

$$E_{\text{photon}} = E_{\text{photon0}} \left( \frac{\sqrt{1 - (v_{7\text{Li}^{2+}}/c)^2}}{1 - (v_{7\text{Li}^{2+}}/c)\cos\theta} \right). \quad (7)$$

In Eq. (7),  $E_{\text{photon0}}$  is the transition energy and  $c$  is the speed of light. The  $\theta$  represents the angle between the observation line of sight and the  ${}^7\text{Li}^{3+}$  velocity vector. In the VIS range, the emission spectrum is influenced by the fine structure. Therefore, when evaluating the emission spectrum, we must compute the branching ratio of each subshell from the Einstein's A coefficient. Because the spectral line is split by the fine structure, the emission spectrum may spread more widely than that under the Doppler effect alone. Therefore, the calculated emission spectra due to transitions from each subshell were weighted by the branching ratios. The VIS emission spectrum was then obtained by superposing these spectra. The branching ratio was calculated from the Einstein's A coefficient taken from the National Institute of Standards and Technology database [18]. Table 1 lists the parameters used in the analysis. The  $V$  represents the plasma volume.  $E_{\text{NBI}}$  is neutral beam energy.  $P_{\text{NBI}}$  is neutral beam power.

Table 1 Calculation parameters.

Parameter	Value
$E_{\text{NBI}}$ (proton) [keV]	300-1000
$P_{\text{NBI}}$ (proton) [MW]	33
$T_e, T_d$ [keV]	1-5
$n_e, n_d$ [ $\text{m}^{-3}$ ]	$10^{19}$
$n_{6\text{Li}}$ [ $\text{m}^{-3}$ ]	$10^{18}$
$\tau_p$ [s]	6
$V$ [ $\text{m}^3$ ]	800

### 3. Results and Discussion

Figure 2 shows the deuteron velocity distribution functions for different (a) beam energies and (b) plasma temperatures. Changing the beam energy alters the energy region in which the knock-on tail is formed. Moreover, when the beam energy is low, the size of the knock-on tail becomes small. This can be explained by the small NES cross-section at low keV beam energies. The Rutherford differential cross-section is inversely proportional to the fourth power of the relative velocity between particles. When the plasma temperature (both ion temperature and electron temperature) is low, the relative velocity between the electron and the recoiled deuteron decreases, so that the collision frequency of Coulomb scattering with the electron increases. Therefore, the slowing-down of the recoiled deuteron by electrons is enhanced. On the contrary, the relative velocity of bulk deuteron and recoiled deuteron increase when the plasma temperature is low. Therefore the slowing-down of recoiled deuteron by bulk deuteron is suppressed. The energy of the recoiled deuterons is sufficiently higher than that of the bulk deuteron, and the slowing-down of recoiled deuterons is

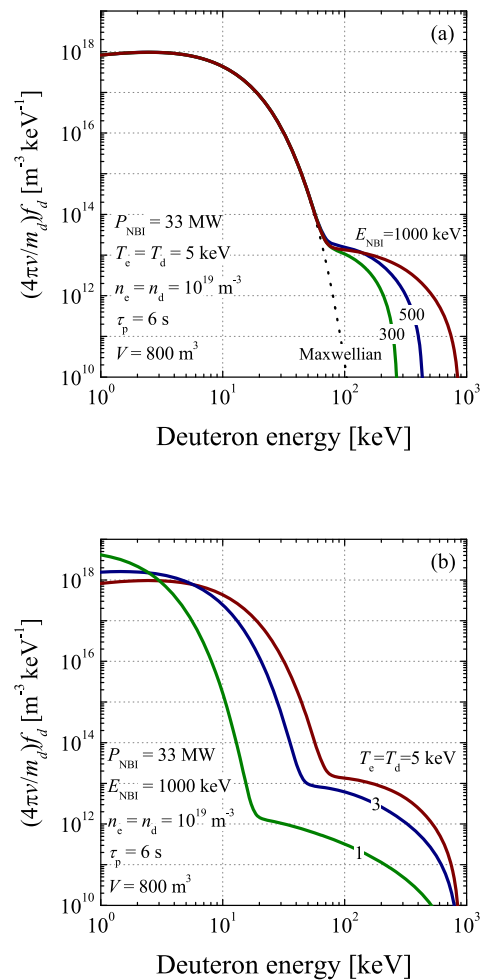


Fig. 2 Deuteron velocity distribution functions for different (a)  $E_{\text{NBI}}$ , (b)  $T_e$  and  $T_d$ .

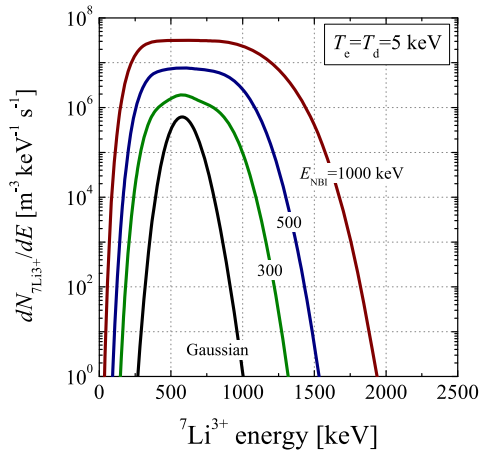


Fig. 3  ${}^7\text{Li}^{3+}$  energy spectra when  $T_e = T_d = 5$  keV.

dominated by Coulomb scattering with electrons. Therefore, decreasing the plasma temperature works to reduce the size of the knock-on tail.

Figure 3 shows the  ${}^7\text{Li}^{3+}$  energy spectra at different beam energies when  $T_e = T_d = 5$  keV. If the deuteron velocity distribution function is Maxwellian, the  ${}^7\text{Li}^{3+}$  energy spectrum is close to the Gaussian distribution. When the knock-on tail is formed, the maximum value of the  ${}^7\text{Li}^{3+}$  energy spectrum increases from a few times to several dozen of times. As shown in Fig. 1, the cross-section of the  ${}^6\text{Li}+d$  reaction increases in the high energy region, meaning that the energy rate of  ${}^7\text{Li}^{3+}$  increases. The energy spectrum is also greatly distorted from a Gaussian distribution, and flattens, especially in the 250 - 1000 keV region at  $E_{\text{NBI}} = 1000$  keV. When the beam energy is high, the bulk deuteron reacts less than the energetic deuteron. Hence, the Gaussian component of the  ${}^7\text{Li}^{3+}$  energy spectrum is not dominant. In addition, the spectrum at  $E_{7\text{Li}^{3+}} = 1000$  keV shows a 7-digit higher order of magnitude than that for the Gaussian distribution.

Figure 4(a) shows the normalized VUV emission spectrum (expected) when  $T_e = T_d = 5$  keV and  $E_{\text{NBI}} = 1000$  keV. Figure 4(b) is an enlargement of the upper wavelength part of the normalized emission spectrum. The full width at half maximum is little changed by the knock-on tail formation, indicating that the Doppler broadening significantly changed only in the fast component. From this result, we defined the basic physical quantity of our evaluation, namely, the  $\Delta\lambda$  specifying the wavelength difference between the cases with and without the knock-on tail where the intensity has declined by  $1/e^2$  of the maximum. Under the conditions of Fig. 4,  $\Delta\lambda$  is approximately 0.03 nm. A similar tendency is observed in the expected VIS emission spectra. As the Doppler broadening is sufficiently large, the expected emission spectra are not distorted by the fine structure.

Figure 5 shows the beam energy dependencies of the  $\Delta\lambda$  in the (a) VUV and (b) VIS spectra. In Fig. 5, the  $\Delta\lambda$

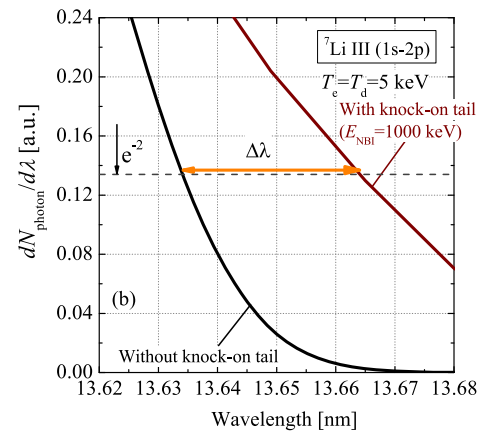
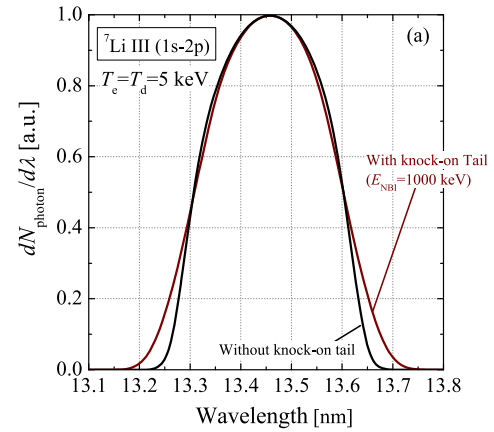


Fig. 4 (a) Normalized VUV emission spectra (expected) of  ${}^7\text{Li}^{2+}$  in the case of  $T_e = T_d = 5$  keV and  $E_{\text{NBI}} = 1000$  keV, (b) enlarged view.

becomes large at higher beam energies. This is because the distortion from the Gaussian distribution increased with increasing beam energy (see Fig. 3). Moreover, when the particle velocities are fixed, the Doppler broadening depends only on  $E_{\text{photon0}}$  as shown in Eq. (7). The Doppler broadening is thus larger in the VIS spectrum (with long wavelength) than in the VUV spectrum (with short wavelength). In both the VUV and VIS ranges,  $\Delta\lambda$  does not change greatly with plasma temperatures. Plasma temperatures are not the influential parameters for the  $\Delta\lambda$  because  ${}^7\text{Li}^{3+}$  generation energy is much higher than plasma temperatures. Next we compare the  $\Delta\lambda$  and the wavelength resolution of the current spectrometer. The VUV spectrometer on the Large Helical Device is resolved to approximately 0.01 nm [19]. At the beam energy of 500 keV or higher, the  $\Delta\lambda$  can be measured at any plasma temperatures. At  $E_{\text{NBI}} = 1000$  keV, the  $\Delta\lambda$  is approximately three times larger than the wavelength resolution of the spectrometer. The  $\Delta\lambda$  is enough for the knock-on tail observation. Conversely, at a beam energy of 300 keV, measurement is difficult. In the VIS range, the resolution of the spectrometer on the Large Helical Device is approxi-

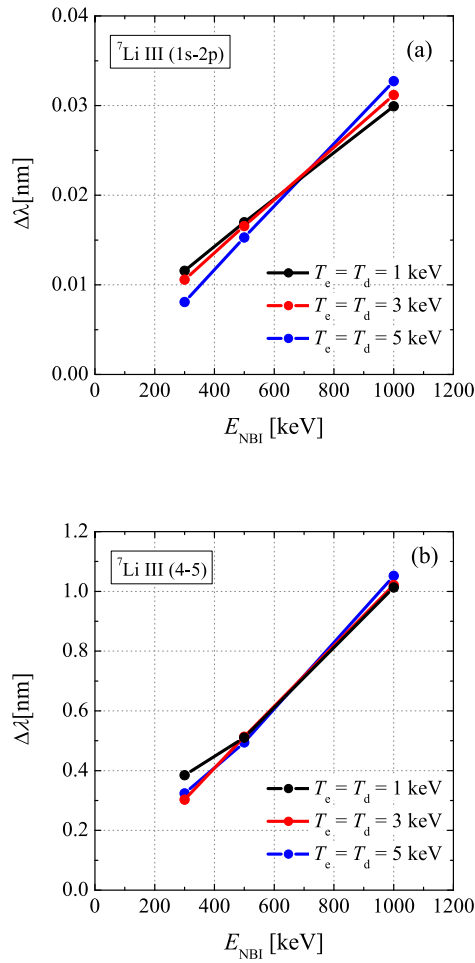


Fig. 5 Dependencies of wavelength difference  $\Delta\lambda$  between the cases with and without the knock-on tail on the beam energy with  $T_e$  and  $T_d$  as a parameter in (a) VUV and (b) VIS spectra.

mately 0.004 nm [20], which is sufficient for detecting the  $\Delta\lambda$  at any beam energies in the VIS spectrum.

Figure 6 shows the beam energy dependencies of emissivities per unit solid angle in the (a) VUV and (b) VIS spectra. When the beam energy is 500 keV or higher, emissivities per unit solid angle are saturated. Because decrement of the fast neutral hydrogen and increment of  ${}^7\text{Li}^{3+}$  densities with increasing beam-injection energy are approximately canceled, this tendency is caused by the cross-section of the charge-exchange reaction. The cross-section becomes roughly constant in low relative-energy range between fast neutral hydrogen and  ${}^7\text{Li}^{3+}$ , and rapidly decreases as the relative energy increases. When we focus our attention on the  ${}^7\text{Li}^{3+}$ s with 1 - 1.5 MeV energy (who are strongly reflected the knock-on tail formation), the charge-exchange cross-section gradually increases and saturates as the beam energy increases and reaches 1 - 1.5 MeV energy range, i.e., as the relative energy is close to zero. Decreasing the plasma temperature lowers emissivities per unit solid angle by one to two orders of magnitude. This is because the  ${}^6\text{Li}+\text{d}$  reaction rate

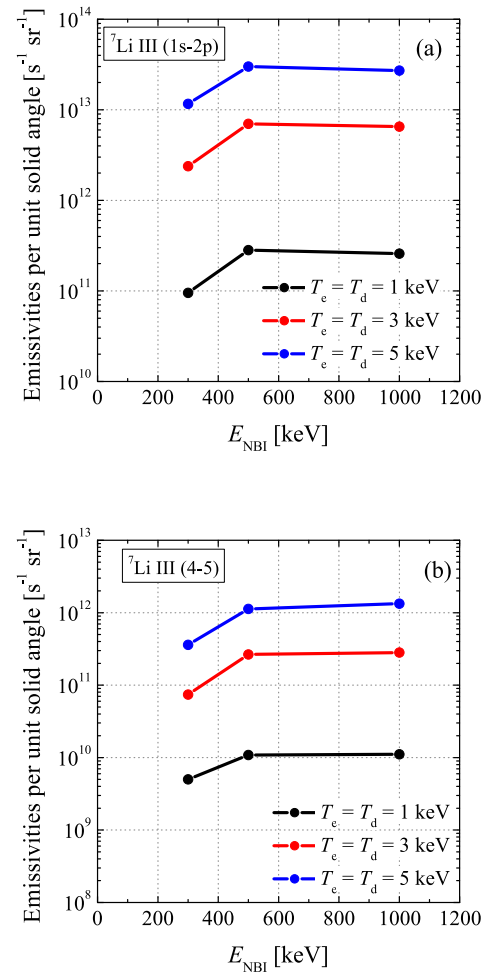


Fig. 6 Emissivities per unit solid angle at  $T_e$  and  $T_d$  in (a) VUV and (b) VIS spectra.

decreases and the amount of  ${}^7\text{Li}^{3+}$  existed in the plasma decreases.

Throughout the simulations, we assumed a uniform plasma. The temperatures, densities and hydrogen beam (energetic proton) in actual plasma have spatial distributions. To select the line of sight of the spectrometer, it is necessary to carry out the simulations considering the spatial distributions.

## 4. Conclusion

This paper shows a possibility of Doppler broadenings of the VUV and VIS emission spectra of the energetic  ${}^7\text{Li}$  produced by  ${}^6\text{Li}+\text{d}$  reaction to observe the knock-on tail on the deuteron velocity distribution function. The VUV and VIS spectra for the cases when a knock-on tail is formed and not formed in hydrogen beam injected deuterium plasma were evaluated. In particular, the Doppler broadening of the VIS spectrum is sufficiently larger than the resolution of the current spectrometer, and a detailed observation of the size and shape the knock-on tail can be expected. Because emissivities per unit solid angle

strongly depend on the plasma temperature, we must determine suitable plasma conditions for the observation. The  ${}^6\text{Li}+d$  reaction can also produce  ${}^7\text{Be}$ . As the reaction cross-section of  ${}^6\text{Li}(d,n\gamma){}^7\text{Be}$  is approximately equal to that of  ${}^6\text{Li}(d,p\gamma){}^7\text{Li}$ , the emission spectrum of  ${}^7\text{Be}$  would also be available for the knock-on tail observation. Another conceivable option is the emission spectrum of  ${}^3\text{He}$  produced by the DD reaction. These alternative candidates will be investigated in future works.

- [1] J.J. Devaney and M.L. Stein, Nucl. Sci. Eng. **46**, 323 (1971).
- [2] S.T. Perkins and D.E. Cullen, Nucl. Sci. Eng. **77**, 20 (1981).
- [3] L. Ballabio, G. Gorini and J. Källne, Phys. Rev. E **55**, 3358 (1997).
- [4] J. Källne, L. Ballabio, J. Frenje *et al.*, Phys. Rev. Lett. **85**, 1246 (2000).
- [5] H. Matsuura and Y. Nakao, Phys. Plasmas **14**, 054504 (2007).
- [6] Y. Nakao, H. Matsuura, T. Hanada *et al.*, Nucl. Fusion **28**, 1029 (1988).
- [7] H. Matsuura *et al.*, Plasma Fusion Res. **2**, S1078 (2007).
- [8] S. Hirayama, H. Matsuura and Y. Nakao J. Plasma Fusion Res. SERIES **8**, 662 (2009).
- [9] H. Matsuura *et al.*, Fusion Sci. Technol. **60**, 634 (2011).
- [10] H. Matsuura *et al.*, Plasma Fusion Res. **8**, 2403064 (2013).
- [11] R.J. Fonck *et al.*, Phys. Rev. A **29**, 3288 (1984).
- [12] D. Ryutov, Phys. Scr. **45**, 153 (1992).
- [13] P. Helander *et al.*, Plasma Phys. Control. Fusion. **35**, 363 (1993).
- [14] J.D. Gaffey, J. Plasma Phys. **16**, 149 (1976).
- [15] V.T. Voronchev *et al.*, Mem. Fac. Eng. Kyushu Univ. **51**, 63 (1991).
- [16] M.J. Singh *et al.*, New J. Phys. **19**, 055004 (2017).
- [17] <https://dbshino.nifs.ac.jp>
- [18] <http://physics.nist.gov/PhysRefData/ASD/>
- [19] C. Suzuki *et al.*, J. Phys. Conf. Ser. **163**, 012019 (2009).
- [20] M. Goto *et al.*, Fusion Sci. Technol. **58**, 394 (2010).